DOI: 10.1002/zaac.201300269

Phase Chemistry in the Ca-Mn-Sb-O System at 1160–1250 °C

Gennady V. Bazuev,*[a,b] Aleksander P. Tyutyunnik,[a] and Boris G. Golovkin[a]

Keywords: Phase equilibrium; Oxides; Chemical synthesis; Crystal structure; Manganese; Antimony

Abstract. Phase equilibrium in the Ca-Mn-Sb-O system was studied in air at the temperature range from 1160 to 1250 °C and a pseudo-quaternary phase diagram for the system CaO-MnO-Mn_2O_3-Sb_2O_5 is presented. The following compounds were discovered: new antimonate $Ca_7Sb_2O_{12}$ with a perovskite-like structure, solid solutions $Mn_{2-x}Ca_xSb_2O_7$ ($0 \le x \le 1.6$) with a 3*T*-weberite structure, and $Ca_{2-x}Mn_xSb_2O_7$ ($0 \le x \le 0.23$) with a 2*O*-weberite structure, as well as solid solutions $Ca_2Mn_{1+x}Sb_{1-x}O_6$ with monoclinic ($0 \le x \le 0.67$) and orthorhombic ($0.75 \le x \le 1$) perovskite structures. The existence of a number of double and ternary oxides and solid solutions on the basis of Sb^{5+} and Mn^{2+}, Mn^{3+}, Mn^{4+} and with mixed manganese valence is confirmed.

Introduction

Chemical phase diagrams are the most convenient form of representation, the description and storage of information on results of researches of interaction in multicomponent oxides systems. They are a basis of the directed synthesis of ternary oxides compounds as allow unambiguously and visually to define conditions of phase equilibriums, formation of new phases in system, emergence and dissociation of solid solutions. It makes sense to describe multicomponent systems on the basis of experimental studies of interactions in quasidouble systems in aggregate with the thermodynamic analysis of state diagrams. In the absence of thermodynamic characteristics of the phases making system, the results of experimental studies are a basis for the description of system.

A large number of binary and ternary oxides, as well as solid solutions (SS) of different composition were found to form in the quasi-ternary system Ca-Mn-Sb-O under usual conditions. Characteristic of this system is the multivalent state of manganese. In the ternary oxides forming this system, manganese exists in the form of Mn^{4+}, Mn^{3+}, and (or) Mn^{2+} cations, and antimony exists mainly as Sb^{5+}.[1–6] Such various oxidation states of manganese characteristic for a wide interval of temperatures, apparently, are defined by the chemical nature of oxides of manganese (II), (III) and (IV), calcium, and antimony as components of chemical reactions.

This system arouses considerable interest since many binary and ternary oxides of Ca, Mn, and Sb exhibit various physicochemical and physical properties and serve as the basis for developing functional materials for different applications. The antimony pentoxide Sb_2O_5 is used in the production of glasses, ceramics, paints, in textile and rubber-processing industries, as well as in the manufacture of fluorescent daylight lamps etc.[7–10] The complex antimony oxides K(Na)$SbWO_6$ and Bi_3SbO_7 with a pyrochlore structure,[11,12] which are characterized by a high degree of disorder of their cation and anion sublattices, are promising ion exchangers and ionic conductors. Ionic conduction is also typical of the perovskite-like oxide $Sr_{0.5}CaSb_{0.5}O_{3-x}$[13,14] owing to a high level of oxygen vacancies in this compound.

Complex manganese oxides attract attention due to a variety of magnetic, electrical, catalytic, and other properties. Perovskite-like oxides with mixed manganese valence form a large class of magnetoresistive materials. In particular, the doped calcium manganite $CaMn_7O_{12}$ exhibits colossal magnetoresistance[15] provoking undiminishing interest in this and structurally related phases. Recently, it was shown[16] that $CaMn_7O_{12}$ belongs to a class of multiferroics, in which ferroelectric polarization coincides with a magnetic phase transition at 90 K. $CaMn_2O_4$ is reported[17] to be an attractive non-precious catalytic material alternative to traditional Pt/C catalysts for the oxygen reduction reaction, which may find potential applications in alkaline fuel cells and metal-air batteries.

The purpose of this work – specification available and obtaining new information on the crystal chemistry of ternary Ca, Mn, and Sb oxides and phase equilibriums in private double and threefold systems on their basis, research of possible opening of new phases with useful properties.

Brief Overview of Compounds in the Ca-Mn-Sb-O System

The double system CaO-MnO_x is represented by the following Mn^{4+}-based compounds: $CaMnO_3$, $Ca_2Mn^{4+}O_4$, $Ca_3Mn^{4+}{}_2O_7$, $Ca_4Mn^{4+}{}_3O_{10}$, and $Ca_2Mn^{4+}{}_3O_8$.[1] The stoichiometric perovskite of $CaMnO_{3.00}$ can be received by low-temperature methods,[18] whereas a method of solid-phase reactions leads to formation of oxygen deficient samples of

* Prof. G. V. Bazuev
Fax: +7-343-374 4495
E-Mail: bazuev@ihim.uran.ru
[a] Institute of Solid State Chemistry
Ural Branch of the Russian
Academy of Sciences
620990, Ekaterinburg, GSP, Russia
[b] Ural Federal University
620002, Ekaterinburg, GSP, Russia

$CaMnO_{3-\delta}$. From this row we didn't find data on considerable deficiency of an oxygen sublattice of other manganites.

According to data,[2] $CaMnO_3$ forms a solid solution with the Ca/Mn ratio varying from 2:1 to 1:1. Later, these data have not been confirmed. The former four compounds are stable at high temperatures, whereas $Ca_2Mn_3O_8$ decomposes in air at 810 °C.[1] In the trivalent state, manganese exists in the compound $CaMn_2O_4$, on the basis of which a solid solution is formed at high temperatures. This oxide has a marokite structure and is generally referred to as a post-spinel phase crystallizing in an orthorhombic syngony.[3] At low temperatures, several compounds with mixed manganese valence have been synthesized ($CaMn^{3+}{}_2Mn^{4+}O_6$, $CaMn^{3+}{}_2Mn^{4+}{}_2O_8$, $CaMn^{3+}{}_6Mn^{4+}O_{12}$), which decompose above 840–940 °C.[1]

In the system MnO_x-Sb_2O_x under usual conditions the compounds on the basis of MnO, Sb_2O_3, and Sb_2O_5 oxides are received. $Mn^{2+}Sb_2O_6$ existing in four different modifications[4,19,20,21] and $Mn^{2+}{}_2Sb_2O_7$[20,21] are formed in the Mn-Sb-O system in air. According to the literature,[19] β-$MnSb_2O_6$ begins to decompose above 1100 °C, and at 1335 °C the remainder has the composition $Mn_2Sb_2O_7$ and at ca. 1450 °C Mn_3O_4. α-$MnSb_2O_6$ has a columbite-type structure.[4] Trigonal γ-$MnSb_2O_6$ was registered in mixture with $Mn_2Sb_2O_7$ at 900 °C.[20] $Mn_2Sb_2O_7$ has a trigonal 3*T*-weberite structure above 900 °C[20] (its composition corresponds to the formula $Mn_2Sb_2O_{6.75}$[21]) and a cubic pyrochlore structure.[22] This modification of $Mn_2Sb_2O_7$ was obtained from the acetate $Mn(Ac)_2{\cdot}H_2O$ and antimonite acid $Sb_2O_3{\cdot}H_2O$ in air at 450 °C. The $Mn_{1-x}Sb^{3+}{}_{1+x}O_4$ phase ($0 \le x \le 0.33$) with a rutile structure was synthesized by the sol-gel method; it is stable for 14 h during heating in air to 740 °C and at 800 °C it decomposes with the formation of $MnSb_2O_6$.[23,24] The compound $MnSb^{3+}{}_2O_4$ having a tetragonal Pb_3O_4 type structure and $Mn_3Sb^{3+}{}_2O_6$ were produced under hydrothermal conditions.[25] The naturally occurring mineral manganostibite[26] of the composition $(Mn^{2+},Mn^{4+})Mn_4Sb_2O_{15}$ has an orthorhombic braunite or hausmannite structure. The synthetic analogue of this mineral was not obtained so far.

The interaction between calcium and antimony oxides has not been studied in detail. At present, the compounds $CaSb_2O_6$[5,27] $Ca_2Sb_2O_7$,[4–6] and $Ca_6Sb^{3+}Sb^{5+}O_{10}$[5] were registered in the Ca-Sb-O system during synthesis in air. The formula of the latter compound is written in the literature[28] as $Ca_6Sb^{5+}{}_2O_{11}$. The crystal structure of this compound has not been established. $Ca_2Sb_2O_7$ synthesized at atmospheric pressure has an orthorhombic 2*O*-weberite structure[29] and at a pressure of 6 GPa[6] a cubic pyrochlore structure. Compounds based on Sb^{3+} ($CaSb_2O_4$, $Ca_2Sb_2O_5$, $Ca_4Sb_2O_7$, $Ca_3Sb_2O_6$) and those having mixed degrees of oxidation of Sb^{3+} and Sb^{5+}[5] were obtained at low temperatures without oxidizers or during mechanochemical treatment.[30] With increasing temperature, they decompose into binary oxides based on Sb^{5+}.

In the Ca-Mn-Sb-O system, two ternary compounds have been described: the binary perovskite $Ca_2Mn^{3+}SbO_6$ obtained in works[31–35] and the mineral ingersonit $Ca_3Mn^{2+}Sb_4O_{14}$ identified in reference[36]. $Ca_3Mn^{2+}Sb_4O_{14}$ is isostructural with $Mn_2Sb_2O_7$ and has a trigonal 3*T*-weberite structure. States of oxidation of Mn and Sb in these compounds are confirmed with structural researches, X-ray absorption spectroscopic data and magnetic measurements.[31–35]

Up to now, the phase diagram of the Ca-Mn-Sb-O system has not been examined. Since compounds in this system contain Mn and Sb in different (including mixed) degrees of oxidation, it is necessary to determine their stability regions. For this purpose, phase equilibria diagrams are usually used. In the ternary system Ca-Mn-O, the phase relationships were studied in detail in air in the temperature range from 700 to 2600 °C.[1] The introduction of antimony considerably complicates the composition of this quasi-ternary system because of inclusion of binary ($Ca_xSb_yO_z$, $Mn_xSb_yO_z$) and ternary ($Ca_xMn_ySb_zO_m$) oxides and some solid solutions into this system. As some binary compounds of Mn and Sb and Ca and Sb are formed and exist only at low temperatures, the analysis of the Ca-Mn-Sb-O system in this study is limited only to high temperatures.

In the presented work, we tried to generalize the known phases in the Ca-Mn-Sb-O system, as well as the new phases synthesized by the authors, and to represent them as a pseudo-quaternary phase diagram in the temperature range from 1160 to 1250 °C.

Experimental Section

Calcium carbonate $CaCO_3$ and oxides Sb_2O_3 and MnO_2 containing minimum 99.9 % of the main substance were used for sample preparation. The initial reagents were thoroughly mixed, ground, and pressed under pressure 3000 kg·cm^{-2}. The samples were synthesized in a KO-14 electric furnace by stepwise annealing in the temperature range from 900 to 1250 °C. Due to the high volatility of Sb_2O_3 oxide heating of samples was carried out by with a step size of 100 °C. The calcinations process for the samples was performed until specimens reached equilibrium. The phase composition of binary and ternary systems and the purity of the synthesized products were checked using X-ray powder diffraction (XRD) with a Shimadzu XRD-7000 S diffractometer. The crystal structure refinement was carried out with the GSAS[37] program suite using the XRD data. The XRD pattern was collected at room temperature with a STADI P (STOE) diffractometer in transmission geometry with a linear mini-PSD detector using Cu-$K_{\alpha 1}$ radiation in the 2θ range 2° to 120° with a step of 0.02°. Polycrystalline silicon [a = 5.43075(5) Å] was used as external standard. The content of oxygen in the samples received by us determined by a method of iodometric titration (in case samples contained antimony), or restoration in hydrogen current at 900 °C. At discussion of the oxygen content in the phases described in article the data published in original researches also were used.

Results and Discussion

A section of the phase diagram of the system Ca-Mn-Sb-O in air at 1160–1250 °C is shown in Figure 1. The phase diagram corresponding to this system is a tetrahedron with vertices CaO – (MnO_2) – (MnO) – SbO_2+0.5O_2. Bracketed are the conventional components of the system, which do not exist in a given temperature interval, but make it possible to determine the compositions corresponding to figurative points of the system. Accordingly, the conodes, being a part of the coordinates,

Zeitschrift für anorganische und allgemeine Chemie ZAAC Journal of Inorganic and General Chemistry

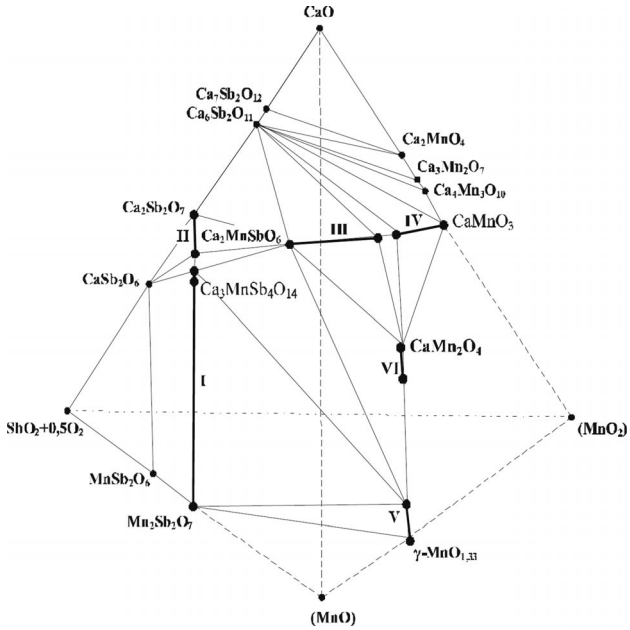

Figure 1. Pseudo-quaternary phase diagram of the system Ca-Mn-Sb-O in air at 1160–1250 °C.

in whose vertices these conventional components lie, are marked with dashed lines. Results of investigations of two pseudo-ternary subsystems represents in Figure 2.

Our experiments confirmed the existence of the three abovementioned compounds ($CaSb_2O_6$, $Ca_2Sb_2O_7$, $Ca_6Sb_2O_{11}$) in the CaO-SbO_x system. Furthermore, the data about the formation of a new compound $Ca_7Sb_2O_{12}$ were obtained for the first time, and its composition was confirmed by structural studies. This compound was synthesized from $CaCO_3$ and Sb_2O_3 at 1250 °C. The X-ray diffraction pattern for $Ca_7Sb_2O_{12}$ is demonstrated in Figure 3. The crystal structure of this phase was determined in the space group $P12_1/m1$ to be perovskite-like with monoclinic cell parameters: a = 5.6644(3) Å, b = 5.6655(3) Å, c = 7.9754(2) Å, β = 89.955(4)°. Based on the structural data, we preliminarily have derived the oxygen-deficient formula $Ca(Ca_{0.555}Sb_{0.445})O_{2.667}$. The composition and structure of this phase are close to those of the monoclinic compound $SrCa_{0.3}Sb_{0.7}O_3$[38] [a = 5.7766(2) Å, b = 5.7837(2) Å, c = 8.17183(2) Å, β = 90.039(3)°] in the system Sr-Ca-Sb-O. In the same system, a solid solution of the composition $Sr_{1.45-x}Ca_xSb_{0.55}O_{3-y}$ ($0 \le x \le 1.45$) with a cubic structure was produced in air at 1000 °C.[39] It was noted that at a large concentration of calcium ($x > 1.1$) an impurity phase $Ca_6Sb_2O_{11}$ appears in the samples. The X-ray diffraction pattern of $Ca_7Sb_2O_{12}$ contains a number of peaks of small intensity which can't be attributed to one phase from system CaO-Sb_2O_5. It is probable that these peaks belong to the main phase and testify to additional distortion or ordered of atoms or oxygen vacancies. Further researches of crystal structure this phase by a method of electronic diffraction and high resolution electron microscopy are necessary for definition of a true unit cell this compound.

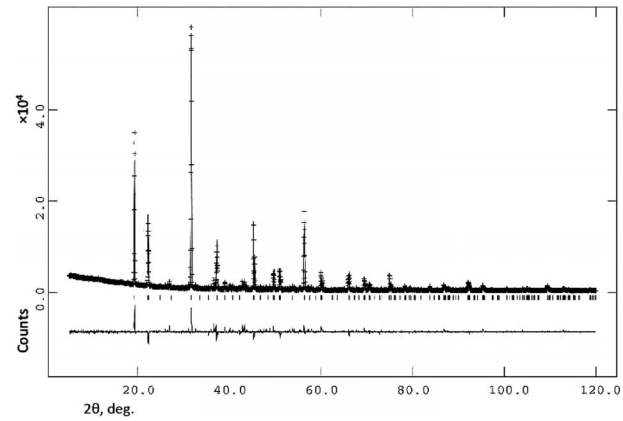

Figure 3. The X-ray diffraction pattern for $Ca_7Sb_2O_{12}$ at room temperature.

As seen from the phase equilibrium diagram (Figure 1, Figure 2), in the Ca-Mn-Sb-O system there exist several solid solutions based on binary and ternary compounds. The first (I) series of SS ($Mn_{2-x}Ca_xSb_2O_7$) is formed on the basis of the $Mn_2Sb_2O_7$ compound with a 3*T*-weberite structure, which at x = 3 includes the ingersonite $Ca_3MnSb_4O_{14}$. Taking into consideration the data,[40] the region of existence of this solid solution is limited to $0 \le x \le 1.6$. At the substitution of Ca^{2+} for

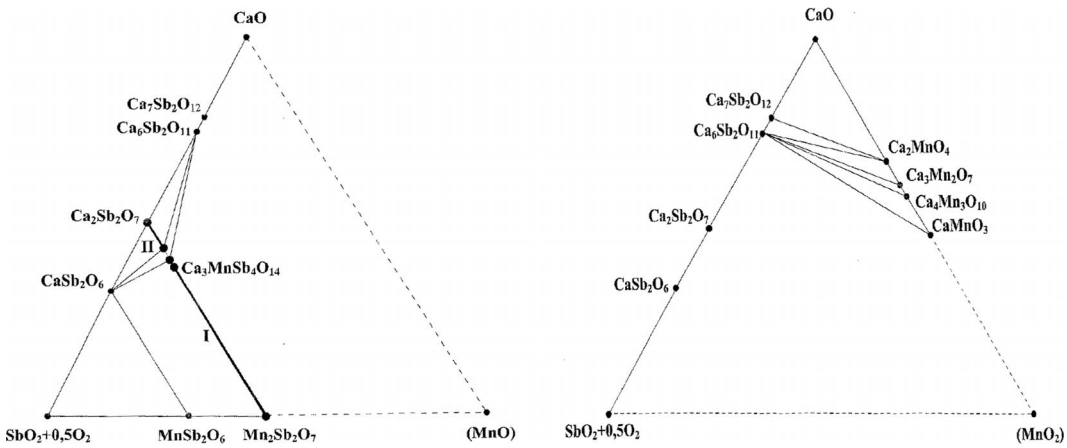

Figure 2. Phase diagrams of CaO-MnO-Sb_2O_5 (on the left) and CaO-MnO_2–Sb_2O_5 (on the right).

Table 1. Units cell parameters of SS $Mn_{2-x}Ca_xSb_2O_7$ (space group $P3_121$).

x	0	0.67	1.00	1.50	1.6 [40]
a /Å	7.193(3)	7.237(2)	7.250(2)	7.280(3)	7.2721(3)
c /Å	17.400 (5)	17.534(4)	17.573 (5)	17.684(3)	17.843 (3)
V /Å^3	779.6(3)	795.35(2)	799.88(4)	811.62(3)	817.18(8)

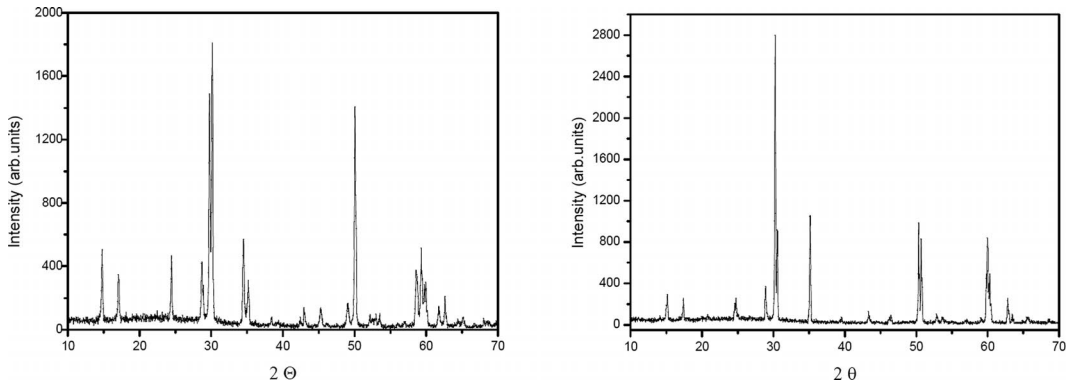

Figure 4. The X-ray diffraction patterns for $Mn_{2-x}Ca_xSb_2O_7$ (x = 1, on the right) and $Ca_{2-x}Mn_xSb_2O_7$ (x = 0.25, on the left).

Mn^{2+}, in accordance with the sizes of these cations (r_{Mn}^{2+} = 0.91 Å, r_{Ca}^{2+} = 1.06 Å[41]), the unit cell parameters increase (Table 1). The second (II) SS is formed by a less extended phase based on $Ca_2Sb_2O_7$:$Ca_{2-x}Mn_x^{2+}Sb_2O_7$ ($0 \le x \le 0.23$)[40] with an orthorhombic 2*O*-weberite structure, which is separated from the SS $Mn_{2-x}Ca_xSb_2O_7$ by a two-phase region. The X-ray diffraction pattern for SS $Mn_{2-x}Ca_xSb_2O_7$ and $Ca_{2-x}Mn_xSb_2O_7$ are demonstrated in Figure 4. The cell parameters of these SS are listed in Table 2.

Table 2. Units cell parameters of SS $Ca_{2-x}Mn_xSb_2O_7$ (space group *Imma*).

x	0.33	0.25	0.00
a /Å	7.2630(2)	7.2873(2)	7.2940(3)
b /Å	10.2031(3)	10.2121(3)	10.2158(4)
c /Å	7.3759(1)	7.423 (2)	7.448(3)
V /Å^3	546.6(3)	552.6(2)	555.0(2)

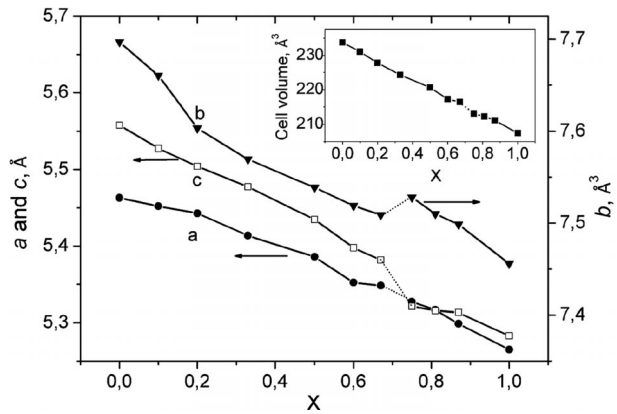

Figure 5. The concentration dependence of the unit cell parameters SS $Ca_2Mn_{1+x}Sb_{1-x}O_6$ with monoclinic ($0 \le x \le 0.67$) and orthorhombic ($0.75 \le x \le 1$) perovskite structures.

From Table 1 follows that parameters a and c of SS $Mn_{2-x}Ca_xSb_2O_7$ (weberite-3*T* type) smoothly increase in an interval $0 \le x \le 1.5$, and at x = 1.6 parameter a decreases, and parameter c increases. Similar change of these parameters is established in the literature[40] for a mineral of $Ca_3MnSb_4O_{14}$ (x = 1.5 in Table 1) and SS $Mn_{0.4}Ca_{1.6}Sb_2O_7$ and caused by features of a crystal structure. In weberite-3*T* there are three independent positions (A1, A2, and A3), which host Mn^{2+} cations in $Mn_2Sb_2O_7$. At replacement of Mn with Ca the last consistently takes A1 and A3 positions. In results Ca^{2+} cations in the mineral Ca_3MnSb_4O[14] are at A1 (distorted cube) and A3 (polyhedron can be described as irregular bicapped octahedron) positions and Mn^{2+} in A2 positions. The atoms of A2 positions are in a tetragonally distorted (2 + 4) octahedron with axial compression along [001]. At x >1.5 A2 positions are occupied by Ca^{2+} cations that leads to anisotropic expansion of the unit cell along [001].[40]

The presence of two perovskite-like compounds (monoclinic $Ca_2Mn^{3+}SbO_6$ and orthorhombic $CaMn^{4+}O_3$) in the examined system allowed us to suppose that either mutual SS or individual compounds with mixed oxidation states of manganese can form on the basis of these compounds. In study[34] some compositions were obtained and it was concluded about the existence of two SS on the basis of $Ca_2Mn^{3+}SbO_6$ and $CaMn^{4+}O_3$. A linear increase of the unit cell volume with increasing antimony concentration was observed for $CaSb_xMn_{1-x}O_3$ (x = 0.1, 0.2, 0.25, 0.33). However, it follows from data[34] that the ratio of the unit cell parameters for the SS of the composition $CaMn_{0.67}Sb_{0.33}O_3$ [a = 5.348(1) Å, b = 7.777(1) Å, c = 5.363(1) Å, β = 90.045(1)°] differs essentially from that for the SS with x = 0.2 and 0.25. This gave us grounds to suggest about possible formation of an individual compound $Ca_3Mn_2SbO_9$.

The synthesis of 11 samples performed in this study in air at 1250 °C confirmed the formation of two series of SS with a perovskite structure in this system: the monoclinic phase of the composition $Ca_2Mn_{1+x}Sb_{1-x}O_6$ (III, $0 \le x \le 0.67$) and the orthorhombic phase (IV, $0.75 \le x \le 1$) (Figure 5, Table 3,

Zeitschrift für anorganische und allgemeine Chemie ZAAC Journal of Inorganic and General Chemistry

Table 3. Unit cell parameters of SS $Ca_2Mn_{1+x}Sb_{1-x}O_6$ (space group $P12_1/m1$).

x	0	0.10	0.13	0.20	0.33	0.50	0.67
a /Å	5.4631(3)	5.4522(2)	5.4509(5)	5.4428(7)	5.4141(4)	5.3867	5.3483(4)
b /Å	7.6969(4)	7.6603(6)	7.6490(6)	7.6034(6)	7.5692(2)	7.5380	7.5101(5)
c /Å	5.5578(5)	5.5276(7)	5.5241(5)	5.5042(8)	5.4773(4)	5.4355	5.3818(2)
β /°	90.21(2)	90.28 (2)	90.29(7)	90.31(6)	91.50 (4)	91.44(3)	90.75(3)
V /Å^3	233.70(5)	231.01(5)	230.32(4)	227.78(5)	224.30 (4)	220.71(3)	216.4(2)

and Table 4). The chemical analysis showed that the content of oxygen in samples close corresponds stoichiometric and is defined by the formula $Ca_2Mn_{1+x}Sb_{1-x}O_{6-\delta}$, where $\delta = 0.04 \pm 0.02$. Existence of similar deficiency of oxygen in these SS is established also in work.[34] These results testify that observed changes of parameters of unit cells and space group SS are mainly caused by replacement of large cations of Mn^{3+} on Mn^{4+} having smaller sizes.

Table 4. Unit cell parameters of SS $CaMn_{1-x}Sb_xO3$ (space group *Pnma*).

x	0 (1)[a)]	0.067 (0.87)[a)]	0.095 (0.81)[a)]	0.125 (0.75)[a)]
a /Å	5.2652(1)	5.2989(2)	5.3169(3)	5.3272(3)
b /Å	7.4559(3)	7.4986(3)	7.5091(4)	7.5281(4)
c /Å	5.2830(2)	5.3134(2)	5.3158(3)	5.3214 (4)
V /Å^3	207.39(3)	211.12(2)	212.35(2)	213.1(4)

a) For formula $Ca_2Mn_{1+x}Sb_{1-x}O_6$.

The X-ray diffraction pattern of $Ca_2Mn_{1.33}Sb_{0.67}O_6$ was indexed on the basis of the monoclinic cell with space group $P12_1/m1$ (No. 11), $Z = 4$, and parameters $a = 5.4137(3)$ Å, $b = 7.5695(5)$ Å, $c = 5.4775(3)$ Å, $\beta = 91.511(2)°$, $V = 224.384$ Å^3. The structure of $CaMn_{0.75}Sb_{0.25}O_{2.93}$[34] was used as starting model for the crystal structure refinement of this phase. The observed, calculated, and difference profiles of X-ray diffraction data refinement for $Ca_2Mn_{1.33}Sb_{0.67}O_6$ are plotted in Figure 6.

The crystallographic data and displacement parameters are given in Table 5, selected interatomic distances in Table 6. It is seen that the parameters and unit cell volumes change smoothly within the $Ca_2Mn_{1+x}Sb_{1-x}O_6$ SS (Figure 5) including the composition $Ca_2Mn_{1.33}Sb_{0.67}O_6$ ($CaSb_{0.33}Mn_{0.67}O_3$ in reference[34]); the parameters of this SS differ essentially from those reported in the literature.[34] Thus, these results show that on the phase equilibrium diagram of the system Ca-Mn-Sb-O the individual compound $Ca_3Mn_2SbO_9$ is absent. In this context, it is interesting that $Ca_3Mn^{2+}Sb_2O_9$ is not formed in this system either, in spite of the existence of the perovskite $Ca_3Co^{2+}Nb_2O_9$.[42] As a whole the results of $Ca_2Mn_{1.33}Sb_{0.67}O_6$ structural refinement testify about a random distribution of manganese and antimony atoms at the 2a and 2c positions. However in the analysis of Table 6 consider-

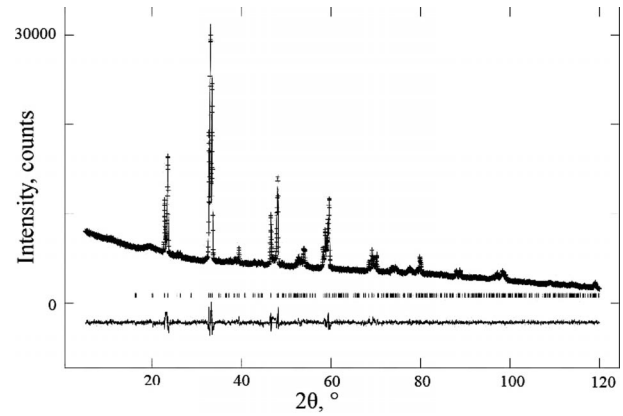

Figure 6. The X-ray diffraction pattern for $Ca_2Mn_{1.33}Sb_{0.67}O_6$ at room temperature.

Table 6. Selected interatomic distances d /Å for $Ca_2Mn_{1.33}Sb_{0.67}O_6$[a)].

Interatomic distances		Interatomic distances	
Ca(1)–O(1)	3.09(3)	Ca(2)–O(1)	2.80(3)
Ca(1)–O(1)	2.43(3)	Ca(2)–O(1)	2.62(3)
Ca(1)–O(2)	2.58(3)	Ca(2)–O(2)	3.03(3)
Ca(1)–O(2)	2.90(2)	Ca(2)–O(2)	2.50(3)
Ca(1)–O(3)	2× 2.93(2)	Ca(2)–O(3)	2× 2.17(2)
Ca(1)–O(4)	2× 2.20(1)	Ca(2)–O(4)	2× 2.34(2)
Ca(1)–O(4)	2× 2.56(1)	Ca(2)–O(4)	2× 2.83(1)
Mn(1)/Sb(1)–O(2)	2× 1.915(4)	Mn(2)/Sb(2)–O(1)	2× 1.905(3)
Mn(1)/Sb(1)–O(3)	2× 2.105(12)	Mn(2)/Sb(2)–O(3)	2× 2.034(12)
Mn(1)/Sb(1)–O(4)	2× 2.152(13)	Mn(2)/Sb(2)–O(4)	2× 1.882(14)
Mn(1)/Sb(1)–O	2.057	Mn(2)/Sb(2)–O	1.940

a) The sum of the effective ionic radii[41]: Mn^{+3} IV HS – 0.645 Å, Mn^{+4} VI HS – 0.53 Å, Sb^{+5} VI –0.63 Å, Ca^{2+} IX 1.18 Å, O^{-2} III – 1.36 Å, O^{-2} IV – 1.38 Å.

Table 5. Atomic coordinates and isotropic thermal parameters[a)] ($U_{iso} \times 100$ /Å^2) for SS $Ca_2Mn_{1.33}Sb_{0.67}O_6$.

Atom		x/a	y/b	z/c	Fraction	Uiso × 100
Ca(1)	2*e*	0.0185(16)	0.25	0.0537(17)	1.0	2.9(3)
Ca(2)	2*e*	0.4770(19)	0.25	0.5197(23)	1.0	5.3(4)
Mn(1)/Sb(1)	2*b*	0.5	0.0	0.0	0.6666/0.3333	3.3(3)
Mn(2)/Sb(2)	2*c*	0.0	0.0	0.5	0.6666/0.3333	2.8(3)
O(1)	2*e*	0.960(5)	0.25	0.492(6)	1.0	4.6(3)
O(2)	2*e*	0.547(5)	0.25	0.974(5)	1.0	4.6(3)
O(3)	4*f*	0.3363(18)	0.012(3)	0.3439(20)	1.0	4.6(3)
O(4)	4*f*	0.1555(21)	0.0455(17)	0.8050(23)	1.0	4.6(3)

a) $wRp = 3.26\%$, $Rp = 2.14\%$, $R(F^2) = 7.89\%$.

able distinctions in average values of interatomic distances of Mn1/Sb2–O and Mn2/Sb2–O in octahedrons (2.057 and 1.94 Å, respectively) attract attention. Considering the sizes of cations of Mn^{3+} (0.645 Å), Mn^{4+} (0.53 Å) and Sb^{5+} (0.60 Å) in octahedral coordination,[41] it is possible to make the assumption that Mn^{4+} cations mainly take in 2c positions.

The analyzed section of the examined phase diagram corresponds to the temperature interval 1160–1250 °C. At 1160 °C, a phase transition from hausmannite γ-Mn_3O_4 to cubic spinel Mn_3O_4 takes place.[1] SS I is equilibrium with $MnSb_2O_6$, $CaSb_2O_6$, SS II of the composition $Ca_{2-x}Mn_xSb_2O_7$ ($0 \leq x \leq 0.23$) with an orthorhombic 2O-weberite structure, as well as with the perovskite $Ca_2Mn^{3+}Sb^{5+}O_6$ and SS V of the composition $Ca_xMn^{2+}{}_{1-x}Mn^{3+}{}_2O_4$ ($0 \leq x \leq 0.23$) with a cubic spinel structure. The perovskite $Ca_2Mn^{3+}Sb^{5+}O_6$ is one of the boundary compositions of SS III based thereon with the general formula $Ca_2Mn_{1+x}Sb_{1-x}O_6$ (III, $0 \leq x \leq 0.67$). The region of the existence of SS III contacts the region of SS IV of the composition $CaMn_{1-x}Sb_xO_3$ (IV, $0 \leq x \leq 0.125$), based on the $CaMnO_3$ perovskite structure in the figurative point of the diagram corresponding to the composition $Ca_2Mn_{1.833}Sb_{0.167}O_6$. SS III, IV, and V are equilibrium with SS VI based on $CaMn_2O_4$ of the composition $Ca_{1-x}Mn_{2+x}O_4$ ($0 \leq x \leq 0.20$). Calcium manganate $CaMnO_3$ is equilibrium with the antimonate $Ca_6Sb_2O_{11}$. The new calcium antimonite $Ca_7Sb_2O_{12}$ is equilibrium with the calcium oxides $Ca_6Sb_2O_{11}$ and Ca_2MnO_4.

The question of the existence of a multivalent state of manganese in isothermal conditions (1160–1250 °C) can be explained on the basis of known inorganic chemistry acid-basic properties of Ca, Mn, and Sb oxides. The basic CaO oxide forms double compounds of Mn^{4+} and Mn^{3+} with subacid MnO_2 oxide and with amphoteric Mn_2O_3 oxide, respectively. The basic MnO oxide reacts with acid Sb_2O_5 oxide. Formation of ternary oxides Ca_2MnSbO_6, $Ca_3MnSb_4O_{14}$, and the solid solutions $Ca_{2-x}Mn_xSb_2O_7$, $Mn_{2-x}Ca_xSb_2O_7$, $Ca_2Mn_{1+x}Sb_{1-x}O_6$ containing Mn^{2+}, Mn^{3+}, and Mn^{4+} cations and a mixture of Mn^{3+} and Mn^{4+} cations can be explained in this way.

Conclusions

(a) In this work generalized known and new phases in the Ca-Mn-Sb-O system are presented in the form of a pseudo-quaternary phase diagram in the temperature range from 1160 to 1250 °C.

(b) In the binary CaO-Sb_2O_5 system the new phase $Ca_7Sb_2O_{12}$ is received for the first time. It is shown that this phase has a monoclinic perovskite structure $Ca(Ca_{0.555}Sb_{0.445})O_{2.667}$, and is characterized by the large number of vacancies in an oxygen subsystem and is of interest to further researches for the purpose of its use as a material with high ionic and electronic conductivity.

(c) The synthesis and crystal chemical analysis of solid solutions with the structures weberite-3*T* ($Mn_{2-x}Ca_xSb_2O_7$), weberite-2*O* ($Ca_{2-x}Mn_xSb_2O_7$), and $Ca_2Mn_{1+x}Sb_{1-x}O_6$ with monoclinic ($0 \leq x \leq 0.67$) and orthorhombic ($0.75 \leq x \leq 1$) perovskite structures is carried out.

(d) The existence in isothermal conditions (1160–1250 °C) of a multivalent state of manganese was explained on the basis of acid-basic properties of Ca, Mn, and Sb oxides.

Acknowledgements

This work was supported by the grant of the Presidium of Ural Branch of the Russian Academy of Sciences (No. 12-P-3–1015).

References

[1] H. S. Horowitz, J. M. Longo, *Mater. Res. Bull.* **1978**, *13*, 1359, and references cited therein.
[2] P. V. Ribaut, A. Maun, *J. Am. Ceram. Soc.* **1963**, *46*, 33.
[3] T. Yang, M. Croft, A. Ignatov, I. Nowik, R. H. Cong, M. Greenblatt, *Chem. Mater.* **2010**, *22*, 5876.
[4] K. Brandt, *Ark. Kemi Mineral. Geol. A* **1943**, *17*, 1.
[5] N. Zenaïdi, R. Renaud, F. A. Josein, *C. R. Acad. Sci. Paris* **1975**, *280*, 1029.
[6] O. Knop, G. Demaseau, P. Hagenmüller, *Can. J. Chem.* **1980**, *58*, 2221.
[7] S. Ezhilvalavan, T. R. N. Kutty, *Appl. Phys. Lett.* **1996**, *68*, 2693.
[8] Y. X. Zhang, G. H. Li, L. D. Zhang, *Chem. Lett.* **2004**, *33*, 334.
[9] Z. T. Deng, F. Q. Tang, D. Chen, X. W. Meng, L. Cao, B. S. Zou, *J. Phys. Chem. B* **2006**, *110*, 18225.
[10] G. Westin, M. Nygren, *J. Mater. Chem.* **1993**, *3*, 367.
[11] Yu. A. Lupitskaya, V. F. Burmistrov, *Russ. J. Inorg. Chem.* **2011**, *55*, 290.
[12] R. Vitlov-Audino, F. J. Linkoln, *Mater. Res. Soc. Symp. Proc.* **1999**, *453*, 561.
[13] E. Chinarro, G. C. Mather, A. Caballero, M. Saidi, E. Moran, *Solid State Sci.* **2008**, *10*, 645.
[14] B. Moreno, E. Urones-Carrote, E. Chinarro, L. Fuentes, E. Moran, *Chem. Mater.* **2011**, *23*, 1779.
[15] Z. Zeng, M. Greenblatt, M. A. Subramanian, M. Croft, *Phys. Rev. Lett.* **1999**, *82*, 3164.
[16] G. Zhang, S. Dong, Z. Yan, Y. Guo, Q. Zhang, S. Yunoki, E. Dagotto, J.-M. Liu, *Phys. Rev. B* **2011**, *84*, 174413.
[17] J. Du, Y. Pan, T. Zhang, X. Han, F. Cheng, J. Chen, *J. Mater. Chem.* **2012**, *22*, 15812.
[18] M. E. M. Jorge, A. C. dos Santos, M. R. Nunes, *Int. J. Inorg. Mater.* **2001**, *3*, 915.
[19] H. Vincent, X. Turrilas, I. Rasines, *Mater. Res. Bull.* **1987**, *22*, 1369.
[20] H. G. Scott, *J. Solid State Chem.* **1987**, *66*, 171.
[21] R. Salmon, M. Graciet, G. Le Flem, *C. R. Acad. Sci. Paris C* **1976**, *282*, 795.
[22] H. D. Zhou, C. R. Wiebe, A. Harter, N. S. Dalal, G. S. Gardner, *J. Phys.: Condens. Matter* **2008**, *20*, 325201.
[23] F. Sala, F. Trifiro, *J. Catal.* **1976**, *41*, 1.
[24] G. Westin, J. Grins, *Acta Chem. Scand.* **1993**, *47*, 1053.
[25] J. R. Gavary, A. W. Hewat, *J. Solid State Chem.* **1983**, *49*, 14.
[26] P. B. Moore, *Arkiv. Miner. Geolog. B* **1967**, *4*, 449.
[27] R. Frank, C. Rocchiccioli-Deltcheff, J. Guillermet, *Spectrochim. Acta Part A* **1974**, *30*, 1.
[28] P. Coursol, N. Stubina, E. Carissimi, M. Zamalloa, P. J. Mackey, *JOM* **2004**, *56*, 41.
[29] F. Brisse, D. J. Stewart, V. Seidl, O. Knop, *Can. J. Chem.* **1972**, *50*, 3648.
[30] V. V. Zyryanov, *Inorg. Mater.* **2003**, *39*, 1163.
[31] E. G. Fesenko, V. S. Filip′ev, M. F. Kupriyanov, R. Devlikanova, G. P. Zhavoronko, V. A. Ochirov, *Izv. AN SSSR Neorganicheskie Materialy* **1970**, *6*, 800.
[32] M. W. Lufaso, P. M. Woodward, J. Goldenberg, *J. Solid State Chem.* **2004**, *177*, 1651.

[33] M. Retuerto, M. J. Martinez-Lope, M. Garcia-Hernandez, A. Nunoz, M. T. Fernandez-Diaz, J. A. Alonso, *Mater. Res. Bull.* **2010**, *45*, 1449.
[34] V. Poltavets, K. Vidyasagar, M. Jansen, *J. Solid State Chem.* **2004**, *177*, 1285.
[35] T. K. Mandal, V. V. Poltavets, M. Croft, M. Greenblatt, *J. Solid State Chem.* **2008**, *181*, 2325.
[36] P. Bonazzi, L. Bindi, *Am. Mineral.* **2007**, *92*, 947.
[37] A. C. Larson and R. B. Von Dreele, "General Structure Analysis System (GSAS)", Los Alamos National Laboratory Report LAUR 86–748, **2004**.
[38] C. C. Luhrs, D. Beltran-Porter, F. Sapina, A. Fuertes, *Int. J. Inorg. Mater.* **2000**, *2*, 483.
[39] M. Saidi, E. Moran, U. Amador, M. Abboudi, A. Asskali, *Mater. Res. Bull.* **2000**, *35*, 1269.
[40] L. Chelazzi, D. Borrini, P. Bonazzi, *Solid State Sci.* **2011**, *13*, 195.
[41] R. D. Shannon, *Acta Crystallogr., Sect. A* **1976**, *32*, 751.
[42] V. Ting, Y. Liu, R. L. Withers, L. Noren, *J. Solid State Chem.* **2004**, *177*, 2295.

Received: May 31, 2013
Published Online: September 13, 2013

